Kontribusi Fisika Indonesia
Vol. 14 No.1, Januari 2003

The Effects of Sinusoidally Modulated Linear Refractive Index on The Wave Characteristics in Linear and Nonlinear Media

Muksin[1,2], R.E. Siregar[1,3], A.A.Iskandar[1#], and M.O. Tjia[1]*
[1]Department of Physics, Institut Teknologi Bandung
[2]Department of Physics, Universitas Syiah Kuala
[3]Department of Physics, Universitas Padjajaran
[#]iskandar@fi.itb.ac.id, [*]fismots@fi.itb.ac.id

Abstract

A numerical study has been carried out on the effects of shallow sinusoidal modulation on the refractive index of linear and nonlinear medium. The result on the linear system demonstrates generally the existence of a transmission band gap at a certain range of wavelength as usually revealed by analytic solution obtained with strictly nonreflecting boundary condition. It is shown in the numerical results that a more general boundary condition leads to similar transmission characteristics as the device length becomes much larger than the modulation period. A further description is given on the variation of gap characteristics with the system parameters. The extension by including the nonlinear term representing the intensity dependent refractive index (IDRI) effect gives rise to a new feature of the transmission gap, exhibiting imperfect reflection characterized by the appearance of transmission channels in the gap. As the input intensity increases, further modification of the gap feature occurs in conjunction with the appearance and growth of hysteretic effect featuring multistable states useful for logic functions. The variations of hysteretic characteristics with respect to the system parameters are also described.

Keywords: *One Dimensional Gratings, Band Gaps, Intensity Dependent Refractive Index, Multistable Nonlinearity*

1. Introduction

The periodic modulation of refractive index of a dielectric medium along the wave propagation direction has been known to result in useful optical devices such as optical filter and reflector. Studies employing the slowly varying envelope (SVE) approximation and spatial averaging (SA) in the case of linear media with shallow modulation and nonreflecting boundary condition have led to an analytical solution of the Helmholtz equation, demonstrating the existence of a transmission band gap[1)]. As this boundary condition is rarely realized in practice, it is interesting and useful to study the consequence of relaxing this boundary condition. For this purpose, a less restrictive boundary condition is introduced, and its effect on the transmission and band gap characteristics are examined numerically.

In order to further explore potentially useful new functions of the system, we have extended the linear case by including a third order nonlinear term arising from the intensity dependent refractive index (IDRI) effect. Restricting our consideration to shallow modulation of both linear and nonlinear refractive index, and working within the SA and SVE approximations, two coupled differential equations have been derived along with two invariant quantities as reported previously by other researchers[2)]. On the basis of these equations, we have further carried out numerical calculation using the more general boundary condition for the determination of the wave transmission characteristics of the periodic system with a number of different system parameters at various input powers. Additionally, we have also studied the hysteretic behavior of the transmitted power with respect to input power, which is expected to arise from the IDRI effect[2)]. The bistable and multistable states associated with this hysteretic behavior are known to promise useful optical logic functions, and the variation of its characteristics is therefore examined with respect to variation of the system parameters.

2. Basic Formulation

The one-dimensional optical periodic system considered is shown in Figure 1, where the refractive indices in the entire region are specified as follows:

$$\begin{aligned} n(z) &= n_0 && ; z \le 0 \\ n(z) &= n_0 + \Delta n(z) && ; 0 \le z \le L \text{ (modulated region)} \\ n(z) &= n_0' && ; z \ge L \end{aligned} \quad (1)$$

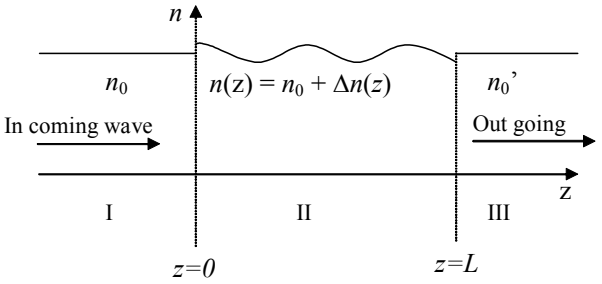

Figure 1. Description of the optical system with periodic modulation of the index in region II.

The refractive indices are assumed to be uniform in the transversal directions. In eq. (1), n_0 and n_0' for region I and region II are constant but not necessarily the same.

The refractive index in region II is assumed to vary sinusoidally along the z direction according to

$$n(z) = n_0 + n_1 \cos(Gz) \tag{2}$$

where $n_1 \cos(Gz)=\Delta n(z)$ in eq. (1), and n_1 is the depth of modulation (modulation index) and G is related to the period of modulation Λ by

$$G = \frac{2\pi}{\Lambda} \tag{3}$$

The depth of modulation n_1 is taken to be much smaller than n_0.

The wave is assumed to propagate in the z direction and no boundary conditions are imposed in the x and y direction. Hence, the wave propagation in each region is governed by the one dimensional Helmholtz equation

$$\frac{d^2}{dz^2}E(z) + k^2 E(z) = 0 \tag{4}$$

with $k = \frac{\omega}{c} n(z)$, c denoting the velocity of light in vacuum and $n(z)$ given by eqs.(1) and (2).

Neglecting n_1^2 with respect to n_0^2 we may rewrite eq.(4) in the following form for region II

$$\frac{d^2}{dz^2}E(z) + \frac{\omega^2}{c^2}\left(n_0^2 + 2n_0 n_1 \cos Gz\right)E(z) = 0 \tag{5}$$

Assuming that the wave is incident from the left, the general solution of eq.(5) can be written as

$$\begin{aligned} &E(z)=A_0 \exp(ik_0 z) + B_0 \exp(-ik_0 z) && ;z \le 0 \\ &E(z) = A(z)\exp(ik_0 z) + B(z)\exp(-ik_0 z) && ;0 \le z \le L \\ &E(z)=A' \exp(ik_0' z) && ;z \ge L \end{aligned} \tag{6}$$

where $k_o=(\omega/c)n_0$. The solution given by eq.(6) satisfies the continuity condition at z=0 and z=L, with $A(z)$ and $B(z)$ representing respectively the forward and backward traveling waves amplitudes. In the following steps, the general solution given by eq. (6) is substituted into eq.(5), which is then reduced to 1st order differentia equation by applying the slowly varying envelope approximation $|A''| \ll |2k_0 A'|$ and $|B''| \ll |2k_0 B'|$. Finally, employing spatial averaging at $2k_0 \cong G$, leads us to two coupled 1st order differential equations for $A(z)$ and $B(z)$ respectively. These equations will be separately discussed in the following for the cases of linear and nonlinear refractive indices.

3. The linear case

The analytical result of this case has been worked out basically by Yeh for specific and restrictive boundary condition[3], but may not be widely known to readers of this journal. It is therefore worthwhile to briefly summarized it here prior to discussions of the more general cases involving less restrictive and hence more practical boundary condition as well as the case involving optically nonlinear medium.

For the linear case, n_0 is independent of E, and the coupled differential equations resulted from the mathematical manipulations described above are given by

$$\frac{d}{dz}A(z) = -i\kappa B(z) e^{i\Delta k z} \tag{7}$$

$$\frac{d}{dz}B(z) = i\kappa A(z) e^{-i\Delta k\ z} \tag{8}$$

where the phase mismatch Δk is

$$\Delta k = 2k_0 - G \tag{9}$$

and the coupling constant

$$\kappa = \frac{\omega n_1}{2c} = \frac{\pi n_1}{\lambda} \tag{10}$$

which denotes the coupling effect between the two counter propagating waves.

By taking $A(z)=|A(z)|\exp(i\phi_a)$ and $B(z)=|B(z)|\exp(i\phi_b)$, then from the two equations one readily obtains two well known invariant quantities, T_c and Γ expressed by

$$|A|^2 - |B|^2 = |T_c|^2 \tag{11}$$

$$\Gamma = |A||B|\cos\psi + \frac{\Delta k}{2\kappa}|A|^2 \tag{12}$$

where $\psi=\phi_a(z)-\phi_b(z)-\Delta kz$.

Upon application of nonreflecting boundary condition $B(L)=0$ as commonly adopted (albeit implicitly), one is led to an analytic solution of the form

$$\begin{aligned} A(z) &= \frac{s\cosh s(L-z) + i(\Delta k/2)\sinh s(L-z)}{s\cosh sL + i(\Delta k/2)\sinh sL} A(0)\exp[i(\Delta k/2)z] \\ B(z) &= \frac{-i\kappa \sinh s(L-z)}{s\cosh sL + i(\Delta k/2)\sinh sL} A(0)\exp[-i(\Delta k/2)z] \end{aligned} \tag{13}$$

where $s = [\kappa^2 - (\Delta k/2)^2]^{1/2}$, which leads to $s=\kappa$ in the case of perfect matching. Further, the analytic expression for the transmittance defined by $T=|A(L)|^2 / |A(0)|^2$ is given by

$$T = 1 - \frac{\kappa^2 \sinh^2 sL}{s^2\cosh^2 sL + (\Delta k/2)^2 \sinh^2 sL} \tag{14}$$

The existence of a transmission gap is clearly indicated by $T=0$ at $s=0$. It is rather straight forward to derive on the basis of eq.(14) and eq.(10) an expression for the gap as follows

$$\Delta\lambda = 2n_1\Lambda \tag{15}$$

which is centered at

$$\lambda_0 = 2n_0\Lambda \tag{16}$$

It is clear from eq.(15) that the gap width increases linearly with n_1 and Λ separately, while the gap center varies linearly with Λ only as indicated by eq.(16).

It is noteworthy that instead of employing the $B(L)=0$ boundary condition, implying the restriction $\Delta n(z)=0$ at $z=L$, we shall henceforth consider a boundary condition specified by the more general relationship

$$B(L)=r(L)A(L) \tag{17}$$

where $r(L)$ is the local *Fresnel* reflection coefficient at z=*L*, which is expressed by

$$r(L) = \frac{n_1 \cos(GL)}{2n_0 + n_1 \cos(GL)} \tag{18}$$

for the case of $n_0' = n_0$. As a consequence, analytic expressions for $A(z)$, $B(z)$ and T given respectively by eqs.(13) and (14) do not hold any longer in this case. Numerical method must be employed in solving for $A(z)$ and $B(z)$ directly from eq.(7) and (8). The resulted solution for $A(z)$ and $B(z)$ in region II are illustrated in Figure 2 for the case of different Δk values at L=300μm. The amplitudes $A(z)$ and $B(z)$ are shown to decay along z direction with B=0 at L=300μm, indicating that the wave is totally reflected at L=300μm for the Δk and Λ=0.5μm considered. However, for the special case satisfying cos(GL)=0 or L=(2m+1)Λ/4 where m=0, 1, 2 etc., we have r=0 at z=L. In this case, the nonreflecting boundary

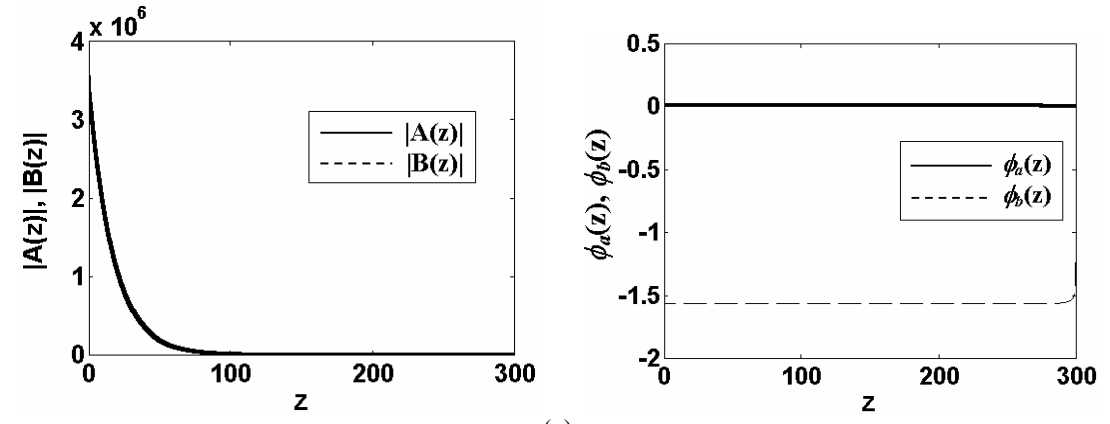

(a)

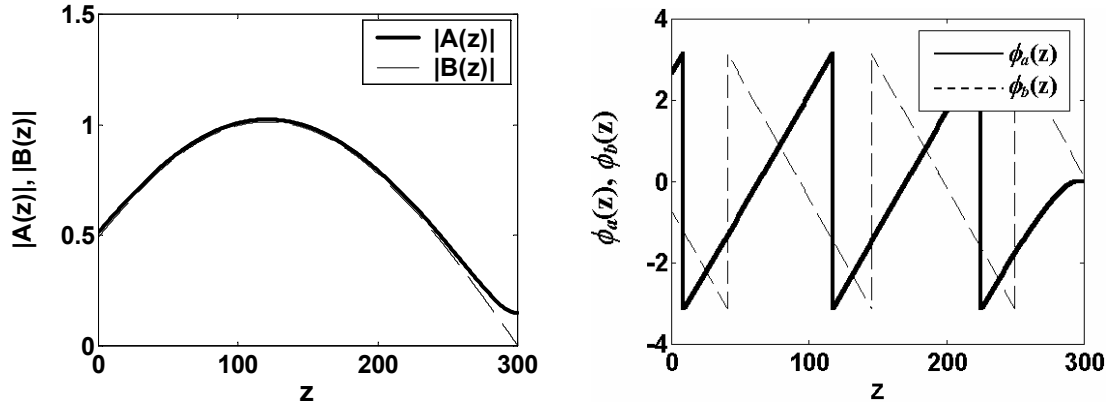

(b)

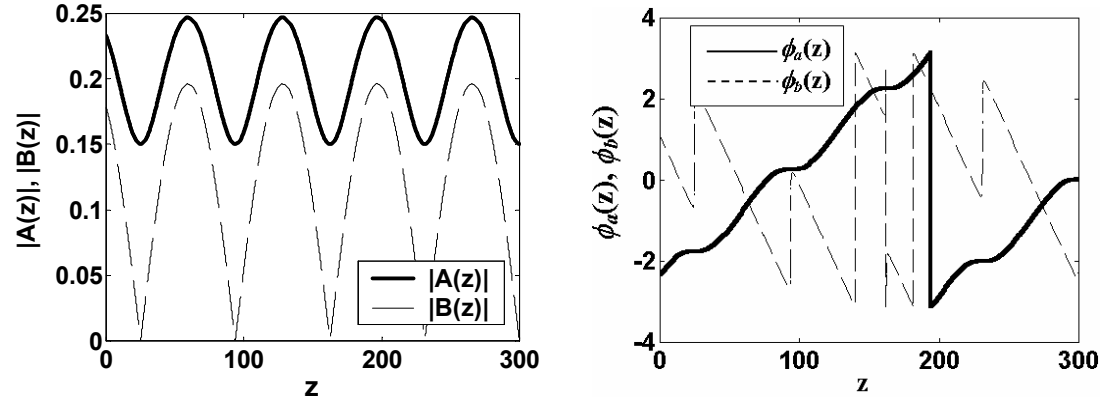

(c)

Figure 2. Graphical representations for the amplitudes and phases of A(z) and B(z) with n_0=2, n_1=0.004, Λ=0.5μm, L=300μm and $|A(L)|$=1V/μm at (a) Δk=0, (b) Δk=0.12μm^{-1}, and (c) Δk=0.15μm^{-1}.

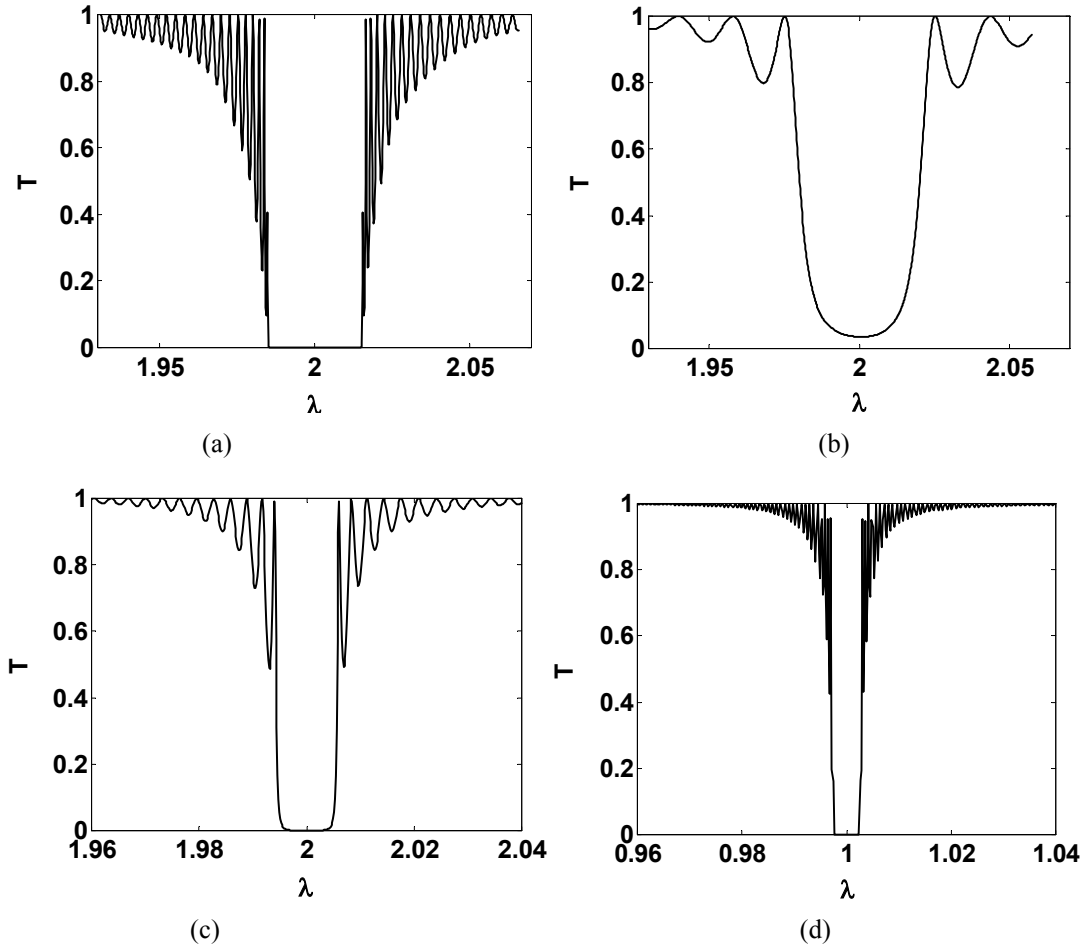

Figure 3. Transmission characteristics exhibiting a band gap obtained numerically for n_0=2 with (a) n_1=0.03, Λ=0.5μm L=300μm. (b) n_1=0.03, Λ=0.5μm, L=50μm. (c) n_1=0.01, Λ=0.5μm, L=300μm and (d) n_1=0.01, Λ=0.25μm, L=300μm.

condition is recovered. It is not difficult to convince oneself that this condition is almost automatically satisfied as long as $L \gg \Lambda$ or $m \gg 1$ as demonstrated numerically in this particular case. It is important to point out from Figures 2(a) and (b) that the rapidly decaying $|A(z)|$ and $|B(z)|$ curves coincide perfectly in the case $\Delta k=0$, while $|B(z)|$ curve lies closely below $|A(z)|$ curve exhibiting non monotonic variation for $\Delta k \neq 0$ (around the gap edge). At even larger value of Δk (further away from the gap center), as shown in Figure 2(c), the curves display non decaying oscillation with the $|B(z)|$ curve lying far below the $|A(z)|$ curves. The corresponding phase function in the first two cases show similar pattern for $|A(z)|$ and $|B(z)|$, but differ considerably in the third cases.

The transmittance as a function of Δk or λ is plotted in Figure 3 for different L, Λ, and n_1. While the existence of a band gap is clearly visible in all cases, a comparison between Figure 3(a) and 3(b) indicates that the gap becomes more sharply defined with near perfect reflection for large L. Comparison between Figure 3(a) and 3(c) demonstrates that a smaller modulation depth leads to a narrower band gap. It is also clear from comparing Figure 3(c) with Figure 3(d) that a smaller Λ results in a shift of the gap center position to smaller λ_0 as well as a narrower gap. These variations of gap characteristics are consistent with the analytic result described earlier. For the more general cases of finite Λ/L, our numerical formulation is expected to offer the desired solution unavailable from the more restrictive analytic formulation.

4. The case with IDRI effect

By taking into account the IDRI effect of the nonlinear medium in region II, the modulated refractive index becomes

$$n(z) = n_o + n_2|E(z)|^2 + n_1 \cos(Gz) \tag{19}$$

Applying the same procedure as employed in the preceding section, we arrive at the following coupled equations:

$$i\frac{dA(z)}{dz} = \kappa B(z)e^{i\Delta kz} + \alpha\left(|A(z)|^2 + 2|B(z)|^2\right)A(z) \tag{20}$$

$$-i\frac{dB(z)}{dz} = \kappa A(z)e^{-i\Delta kz} + \alpha\left(2|A(z)|^2 + |B(z)|^2\right)B(z) \tag{21}$$

where Δk and κ are given by the same expression in eq. (9) and (10) respectively, and the additional parameter is defined by

$$\alpha = \frac{\omega n_2}{c} = \frac{2\pi n_2}{\lambda} \tag{22}$$

which is introduced by the nonlinear effect. The two invariant quantities in this case are given respectively by

$$|A|^2 - |B|^2 = |T_c|^2 \tag{23}$$

which is identical in form with eq. (11) and

$$\Gamma_1 = |A||B|\cos\psi + \left(\frac{3\alpha}{2\kappa}|B|^2 + \frac{\Delta k}{2\kappa}\right)|A|^2 \tag{24}$$

which has the additional term coming from the obvious contribution of nonlinear effect represented by α. The numerical solutions of eq. (20) and (21) and the related transmission characteristics will be described and discussed separately in the following.

4.1 Behaviors *A*(z) and *B*(z)

The calculated results for $A(z)$ and $B(z)$ are presented in Figure 4 for different boundary conditions

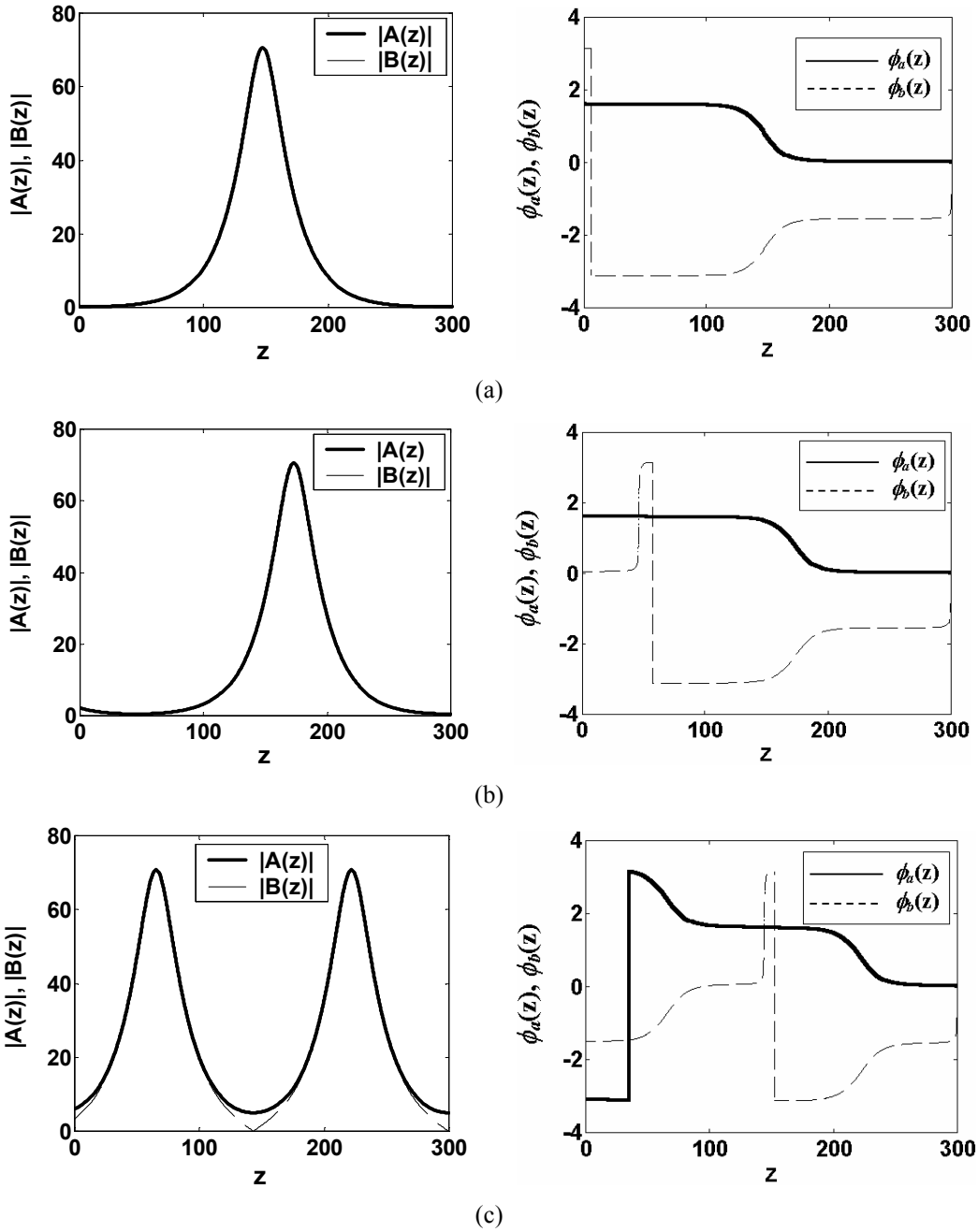

Figure 4. Graphical representations for $|A(z)|$, $|B(z)|$ and $\phi_a(z)$, $\phi_b(z)$ for n_0=2, n_1=0.03, n_2=2x10^{-6}μm^2/V^2, Λ=0.5μm, Δk=0, L=300μm for (a) $|A(L)|$=0.15V/μm, (b) $|A(L)|$=0.5V/μm and (c) $|A(L)|$=5V/μm.

specified by the coefficient of reflection r obtained by assuming $B(L) \ll A(L)$. This assumption is plausibly justified for the case of shallow grating ($n_1 \ll n_0$) and weak IDRI effect ($n_2 \ll n_1$) considered here. The resulted expression for r is given as follows

$$r = \frac{n_1 \cos(GL) + n_2 |A(L)|^2}{2n_0 + n_1 \cos(GL) + n_2 |A(L)|^2} \tag{25}$$

The resulted solution of $|A(z)|$ and $|B(z)|$ for $\Delta k=0$ and L=300μm at different field |A(L)| are plotted in Figure 4(a) and Figure 4(b). It is interesting to note that at a smaller value of $|A(L)|$, the two curves coalesce perfectly. Both the amplitude and the phase display different characteristics from those described in Figure 2. At an intermediate $|A(L)|$, the phases becomes asymmetrically modified, while the field profile remain practically the same. When $|A(L)|$ is further increased, $|B(z)|$ becomes smaller than $|A(z)|$. It is found that this trend continues in the same direction displaying more complicated variations with z when $|A(L)|$ becomes larger. It is also interesting to point out, as will be shown later, that the transmittance characteristics are also clearly affected by the presence of nonlinear property as indicated by their changes with respect to $|A(L)|$.

4.2 Transmittance characteristics

The transmittance curves corresponding to the cases considered in Figure 4 are described in Figure 5. Although the basic feature of a transmission band gap remains visible in those Figure ures, it is also obvious that the gap is now split by the presence of transmission channel in the gap, indicating imperfect reflection in the region. It is shown that for $|A(L)|$=0.15V/μm, the original linear gap admits a single transmission channel at the gap center. For $|A(L)|$=0.5V/μm, two separate transmission channels are allowed in the band gap. Increasing $|A(L)|$ to 6V/μm leads to visible distortion or asymmetry of the gap structure. It is found that the asymmetry is due to the different values of $|A(L)|$ for the same Δk of opposite signs. This difference or distortion which increases with $|A(L)|$ is suspected to have it origin in the nonlinear IDRI effect. It must be added that this enhanced distortion is also accompanied with the appearance of additional transmission channels.

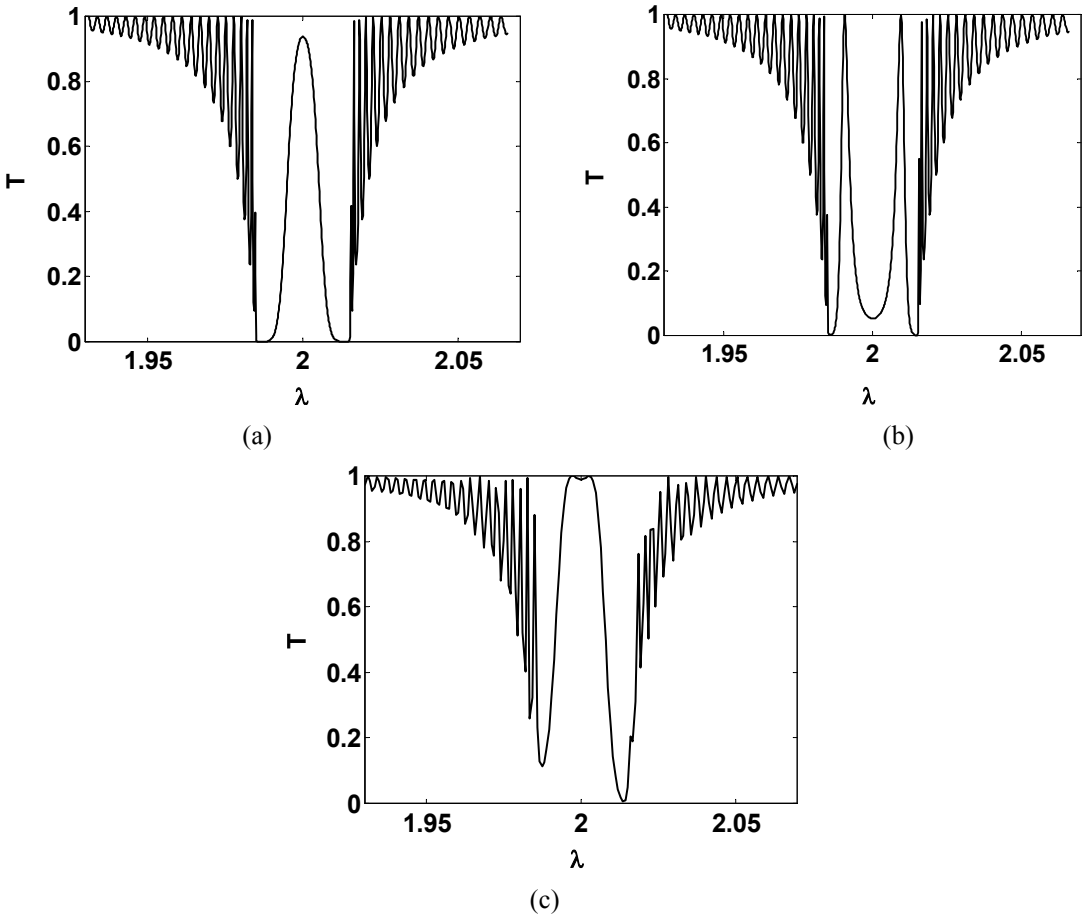

Figure 5. Transmission characteristics of nonlinear system at (a) $|A(L)|$=0.15V/μm, (b) $|A(L)|$=0.5V/μm, and (c) $|A(L)|$=6V/μm showing variation of nonlinearity induces transmission channels in the linear gap due to different input intensities.

4.3 The Optical Multistable and Bistable Feature

For a further study of nonlinear property arising from the IDRI effect, we consider the relationship between the output intensity and the corresponding input intensity. The result of our numerical calculation is shown in Figure 6 which exhibits hysteretic characteristic when the input intensity rises beyond a certain value ($|A(0)|$ is limited to be around 30V/μm by our assumption leading to eq.(25)) as shown in Figure 6(b) and (c). This feature results in the optical bistable states, which seems to "proliferate" at higher input intensity. The hysteretic effect can be characterized by the *hysteresis width* (w_h) and the corresponding turning point I_h indicated in Figure 6(b).

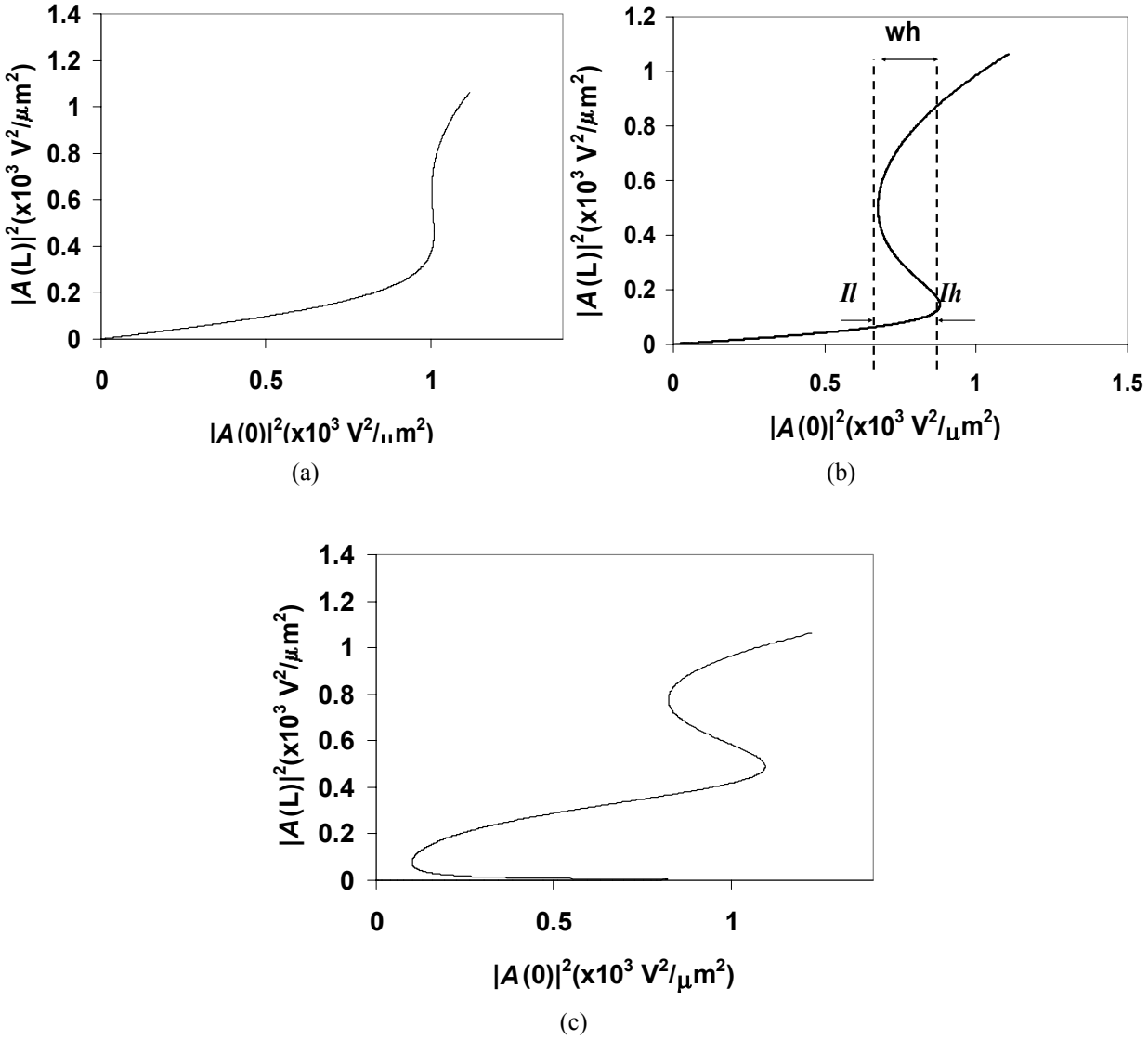

Figure 6. The output intensities $|A(L)|^2$ are plotted as a function of input intensities $|A(0)|^2$ for n_0=2, n_1=0.005, L=300μm, n_2=2x10^{-6}μm^2/V^2, and Δk=0.0005μm^{-1} showing (a) nonhysteretic pattern for Λ=0.65μm, (b) optical bistable pattern for Λ=0.5μm and (c) optical multistable pattern for Λ=0.25μm.

The hysteretic behavior shown in Figure 7 varies with the changes of L, n_1, n_2 and Δk. These variations in term of the hysteretic parameters are summarized in Figure 8. The value of w_h increases linearly with increasing L and n_1. On the other hand, w_h decreases linearly for increasing Λ and n_2, while showing two regions on the w_h – n_2 curve characteristic by different slopes.

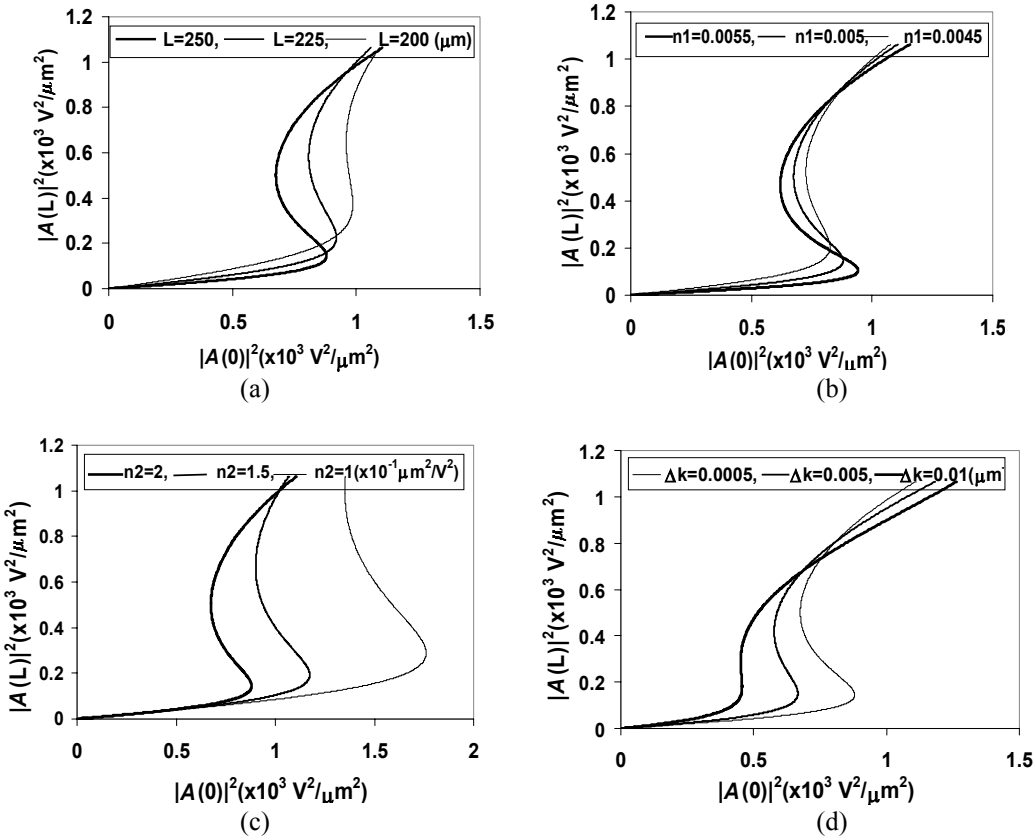

Figure 7. Output power plotted as a function of input power showing the optical bistability with n_0=2 for (a) variation of L, with n_1=0.005, n_2=2x10^{-6}μm^2/V^2, Λ= 0.5μm, and Δk=0.0005μm^{-1}, (b) variation of n_1 with n_2=2x10^{-6}μm^2/V^2, Λ=0.5μm, L=250μm, and Δk=0.0005μm^{-1}, (c) variation of n_2 with n_1=0.005, Λ=0.5μm, L=250μm, and Δk=0.0005μm^{-1} (d) variation of Δk with n_1=0.005, n_2=2x10^{-6}μm^2/V^2, Λ=0.5μm, and L=250μm.

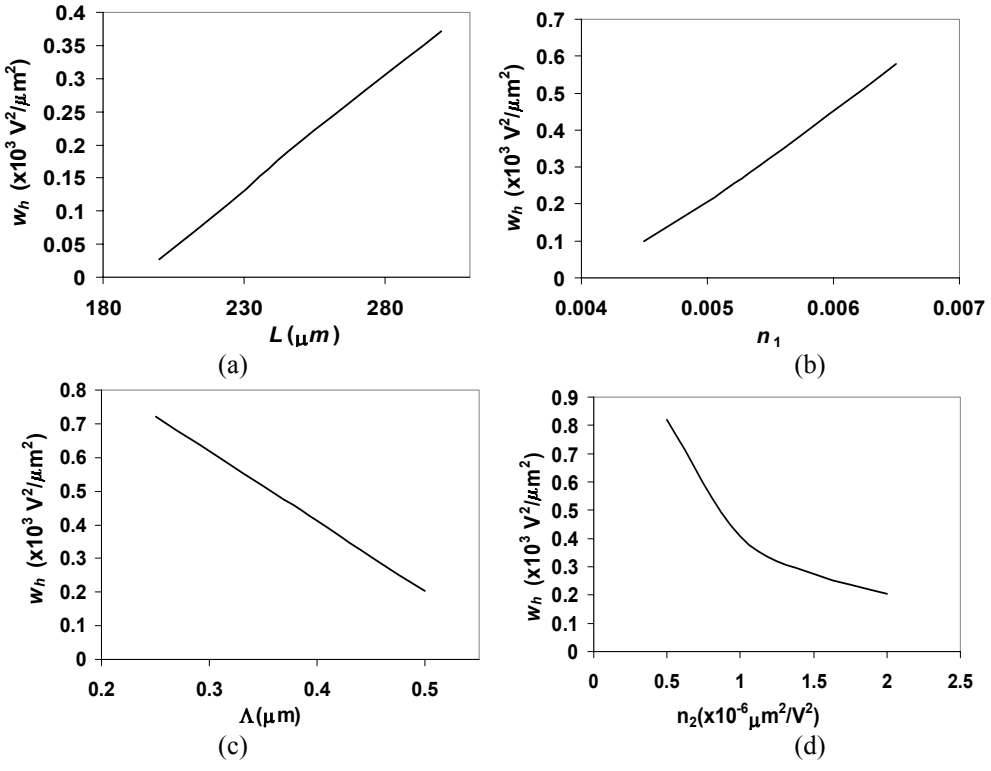

Figure 8. Hysteretic width w_h plotted as a function of (a) L, (b) n_1, (c) Λ and (d) n_2.

5. Conclusion

We have solved the wave equation semi analytically in a linear and nonlinear media with sinusoidally modulated linear refractive index. The result for linear cases demonstrates the existence of a transmission gap and the variations of its width and center position with respect to the system parameters. The numerical solutions for nonlinear cases show the appearance of transmission channels in the linear gap, and increasing channels numbers as well as distortion of the transmission gap at higher intensities. At higher input intensities, the nonlinear property of the medium is shown to induce hysteretic effect leading to multistable state solution with intensity dependent characteristics.

References

1. Winfull, H.G., Marburger, J.H., and Garmire E., *Theory of Bistability In Nonlinear Distributed Feedback Structures*, Appl. Phys. Lett. **35**(5), 1979.
2. D.L. Mills, S.E. Trullinger, *Gap Soliton in Nonlinear Periodic Media*, Phys. Rev. B, **36**, 947, 1997.
3. Yeh, P., *Optical Waves in Layered Media*, John Wiley & Sons Inc., New York, 1988.
4. Boyd, R.W., *Nonlinear Optics*, The Institute of Optics University of Rochester, Academic Press, Inc., New York, 1992.
5. Lee, L.D., *Electromagnetic Principles of Integrated Optics*, John Wiley & Sons, Inc., New York, 1986
6. Lindfield, G. and Penny, G., *Numerical Methods Using MATLAB*, Department of Mechanical Engineering, Aston University, Ellis Horwood, New Jersey, 1995.
7. Muksin, *Efek Modulasi Indeks Bias Linier Terhadap Karakteristik Gelombang dalam Media Linier dan Nonlinier*, Department of Physics, Institut Teknologi Bandung, 2002.
8. Nakamura, S., *Applied Numerical Methods with Software*, The Ohio State University, Prentice Hall, New Jersey, 1991.